Published in final edited form as:
Science. 2016 April 08; 352(6282): aad9822. doi:10.1126/science.aad9822.

Term-seq reveals abundant ribo-regulation of antibiotics resistance in bacteria

Daniel Dar[1], **Maya Shamir**[1], **J R Mellin**[2,3,4], **Mikael Koutero**[2,3,4], **Noam Stern-Ginossar**[1], **Pascale Cossart**[2,3,4], and **Rotem Sorek**[1,*]

[1]Department of Molecular Genetics, Weizmann Institute of Science, Rehovot 76100, Israel

[2]Institut Pasteur, Unité des Interactions Bactéries-Cellules, Paris, F-75015 France

[3]INSERM, U604, Paris, F-75015 France

[4]INRA, USC2020, Paris, F-75015 France

Abstract

Riboswitches and attenuators are *cis*-regulatory RNA elements, most of which control bacterial gene expression via metabolite-mediated, premature transcription termination. We developed an unbiased experimental approach for genome-wide discovery of such ribo-regulators in bacteria. We also devised an experimental platform that quantitatively measures the *in-vivo* activity of all such regulators in parallel, and enables rapid screening for ribo-regulators that respond to metabolites of choice. Using this approach we detected numerous antibiotic-responsive ribo-regulators that control antibiotic resistance genes in pathogens and in the human microbiome. Studying one such regulator in *Listeria monocytogenes* revealed an attenuation mechanism mediated by antibiotic-stalled ribosomes. Our results expose broad roles for conditional termination in regulating antibiotic resistance, and provide a tool for discovering riboswitches and attenuators that respond to novel ligands.

Riboswitches and attenuators are 5'UTR-residing, *cis*-regulatory RNA elements (ribo-regulators) that tune gene expression in bacteria by sensing key metabolites, amino acids, nucleotides and ions (1–6). These RNA elements can regulate the expression of the downstream gene either at the transcription or the translation level. When riboswitches and attenuators control transcription they usually generate a condition-specific, regulated transcriptional terminator, such that termination results in a prematurely aborted transcript whereas read-through generates a full length, productive mRNA (5) (Fig. 1A). In the case of riboswitches, the 5'UTR RNA sensor differentially folds to form a terminator or an antiterminator in the presence or absence of a regulating metabolite, respectively; in attenuators, the formation of a transcriptional terminator is mediated by the rate of translation of an upstream ORF (uORF), as exemplified in the Trp operon (4). Regulation by conditional termination controls key processes in bacteria including core metabolism (7, 8), motility (9) biofilm formation (9, 10), and virulence (11, 12). Riboswitches enable optimization of metabolite production in bacterial expression systems (13, 14), are readily

*Corresponding author: rotem.sorek@weizmann.ac.il.

Europe PMC Funders Author Manuscripts

applicable components for synthetic biology applications (15, 16), and also form potential therapeutic targets for novel classes of antibiotics (17, 18).

Only ~25 classes of naturally occurring riboswitches have been described to date, although it is estimated that hundreds more exist in bacteria (19). Almost all known riboswitches have been discovered via comparative-genomics-based approaches comparing intergenic regions across bacterial phyla (20). Once a conserved 5'UTR is detected, its possible ligand is predicted on the basis of the identity of the downstream gene, and these predictions are then subject to extensive *in-vitro* verification. This approach has identified riboswitches conserved across a wide phylogenetic range (19). However, most of the yet to be discovered elements are predicted to be restricted to specific clades of bacteria, and for such elements current conservation-based approaches are not appropriate (19). We currently lack an experimental method that enables genome-wide discovery of riboswitches and conditional termination regulators. Furthermore, given a metabolite of interest, there is no efficient approach that can identify natural riboswitches or attenuators that sense and respond to it.

Genome-wide mapping of RNA 3' termini via term-seq

We developed an unbiased experimental approach for genome-wide discovery of conditional, regulated transcriptional termination in bacteria. For this, we first mapped all RNA termini that are present in the cell at a given condition. As opposed to eukaryotic RNA, where the presence of the nearly universal polyA tail allows direct reverse transcription priming from the 3' end, the absence of 3' polyadenylation in bacterial mRNAs makes 3' ends mapping challenging (21, 22). We developed an RNA-seq protocol (denoted here 'term-seq') that directly sequences exposed RNA 3' ends in bacteria, yielding a genome-wide map of RNA termini (Fig. 1B) (23). Applying term-seq to a large set of synthetic transcripts mixed in various, predetermined concentrations verified that term-seq accurately reconstitutes the exact 3' end termini in a highly quantitative manner (fig. S1).

We applied term-seq on *Bacillus subtilis* (*B. subtilis*) grown in rich media. The sequencing reads resulting from the term-seq protocol showed >50 fold enrichment for mapping to intergenic regions, implying that sites mapped via term-seq represent native RNA termini existing in the cell (Fig. 1C-D) (23). Associating each gene with its respective term-seq-inferred termination position in the downstream intergenic region led to identification of 1443 transcript termini (Fig. 1E; table S1), the vast majority of which conformed to the sequence and structural features of rho-independent transcriptional terminators (Figs. 1F-G, S2) (23). These results demonstrate the ability of term-seq to map RNA termini to the single-base resolution across the bacterial genome.

A platform for the discovery of genes regulated by conditional termination

We next sought to examine whether term-seq can be used to identify regulated, premature termination events. Genes that are transcriptionally regulated by riboswitches and attenuators will present a premature termination site within their 5'UTR, downstream to the transcription start site (TSS). We therefore also mapped TSSs across the *B. subtilis* genome using a genome-wide 5' end sequencing protocol (23–25), and included standard RNA-seq

coverage data to gain a comprehensive view of the *B. subtilis* transcriptome (Fig. 1E) (23). Examining known *B. subtilis* riboswitches showed reproducible premature termination sites at the 5' UTR, supporting that such sites can be indicative of riboswitch activity (Figs. 2A-B).

To assess the sensitivity of this method in revealing genes controlled by regulated termination, we searched for all genes that contained a reproducible term-seq site within their 5'UTRs (23). This search recovered 49 (92%) of the 53 transcriptional units (TUs) regulated by known riboswitches in the *B. subtilis* genome (Fig. 2C; table S2) (23). Four known riboswitch-regulated genes escaped detection, either because they were under the control of multiple consecutive riboswitches, lacked a mapped TSS, or due to an annotation error that placed the riboswitch within a misannotated ORF (fig. S3). These results therefore show a high sensitivity for our method in mapping riboswitches in a genome-wide manner.

Overall, our search retrieved 82 candidate regulatory elements, of which 64 (78%) were mapped to previously reported elements (Fig. 2C; table S2). In addition to the 49 known riboswitches, we also recovered 11 cases of conditional termination known to be regulated by RNA-binding anti-termination proteins; including TRAP(26), GlpP (27), PyrR (28), and PTS system proteins (29). We also identified one case of known attenuation (30), as well as three elements (the *rimP, Pan* and *vmlR* leaders) predicted as *cis*-regulatory elements in *B. subtilis* but for which the mechanism of regulation is unknown (20, 31, 32).

Since *B. subtilis* is a highly studied model organism it has one of the best annotated genomes in the bacterial domain. Nevertheless, we detected 18 new elements predicted to regulate gene expression by premature termination (Fig. 2C; tables S2-S3). These included predicted regulatory elements upstream of the formate dehydrogenase gene *yrhE* (Fig. 2D); the GMP synthase gene *guaA; yfnI*, a gene responsible for the biosynthesis of the polyglycerolphosphate moiety of lipoteichoic acid; and *yxjB,* a 23S rRNA (guanine748-N1)-methyltransferase predicted to confer resistance to macrolide antibiotics (Fig. 2E). The various functions encoded by the genes associated with the new regulators, and the lack of homology to any known riboswitch or other RNA elements in the RNA family database (Rfam) (33), suggest that these regulatory elements may respond to novel ligands, anti-termination proteins or attenuation principles.

We then applied term-seq on *Listeria monocytogenes* (*L. monocytogenes*), a food-borne pathogen that causes gastroenteritis and can lead to severe sepsis and meningitis in immunocompromised and elderly patients, and abortions in pregnant women (34), and *Enterococcus faecalis* (*E. faecalis*), a causal agent of community and nosocomial infections including endocarditis and bacteremia (35). Similar to *B. subtilis*, in both pathogens term-seq detected most of the known riboswitches that function via regulated termination, as well as predicted novel regulators (Figs. 2C, F-I; tables S4-S5). In *L. monocytogenes*, many of the elements we detected were previously annotated as small RNAs or as potential *cis*-acting regulatory 5'UTRs (25, 36); our data supports that they are indeed *cis*-acting regulators (Figs. 2F-G; table S4). The conditional-termination-based elements we detected regulate genes of diverse functions, including some involved in virulence. For example, deletion of the conditional-termination regulator of *lmo0559*, called *rli31* (Fig. 2F), led to an attenuated

virulence phenotype of *L. monocytogenes* in mouse and butterfly infection models (37). Deletion of *rli31* also led to decreased lysozyme resistance of *L. monocytogenes* in blood (38). These results imply that the termination-based regulatory elements we detected may control multiple physiological- and pathogenicity-relevant processes.

Genome-wide metabolite screening in physiological conditions

While our data uncover multiple cases of new candidate regulators, they do not reveal the metabolites to which these regulators respond. Discovery of the metabolite that controls the activity of a given candidate regulator is a major challenge in the field, and usually involves *in-vitro* structural probing of the regulator in the presence of various candidate metabolites and/or the construction of reporter assays to monitor the activity of the regulator (1–3).

We developed a term-seq based strategy to evaluate multiple possible metabolites across all candidate regulators simultaneously in physiological, *in-vivo* conditions. We reasoned that the presence of the metabolite should alter the open/closed state of the regulator, and that this state can be quantitatively measured as the ratio between the full-length RNA and the short, prematurely terminated form (Fig. 3A). As term-seq directly provides a read-through measure (quantification of short/long transcript ratios) for every expressed regulator in the genome, it enables low-cost, parallel analysis of *in-vivo* regulator activities following the application of any metabolite of interest.

To validate this approach, we grew *B. subtilis* in a defined medium with or without the amino acid lysine. Out of the 82 regulators mapped in *B. subtilis,* only the two known lysine riboswitches showed a significant increase in read-through levels as a result of lysine depletion (Figs. 3B-C; S4). Moreover, depletion of a different amino acid from the medium (methionine, Figs. 3B-C) did not increase the open/closed ratio of the lysine riboswitches, pointing to high specificity in sensing the presence of lysine.

Antibiotic-controlled conditional termination regulates antibiotic resistance genes

As inducible antibiotic resistance mechanisms pose a major medical challenge, we screened for regulators that respond to the presence of antibiotics. The rRNA methylase gene *ermK* confers resistance to macrolide-lincosamide-streptogramin B antibiotics and is controlled by conditional premature termination that is alleviated when the antibiotic is introduced (39). Reports have described similar regulation in additional antibiotics resistance genes, but this mode of regulation was considered rare (30, 32). We thus, searched for antibiotic-responsive regulators by applying term-seq to *B. subtilis*, *L. monocytogenes* and *E. faecalis* following short exposure to sublethal doses of seven different antibiotics (table S6) (23). Strikingly, six of the regulators we identified (table S2-S5) showed an antibiotic-dependent response, characterized by read-through into the downstream gene in the presence of the antibiotic (Figs. 4, S5).

Two antibiotic-responsive, termination-based regulatory elements were observed in each of the three bacteria studied. In *B. subtilis*, we identified the *vmlR* (32) and *bmrB* (30)

regulators, which regulate the expression of antibiotic resistance genes through an unknown or ribosome-mediated mechanism, respectively (Figs. 4A-B). In *L. monocytogenes*, however, we discovered two new regulators that were previously annotated as conserved *Listeria* small RNAs of unknown function, *rli53* and *rli59*, and were hypothesized to act in *cis* (36). We found that these two sRNAs function as antibiotic responsive ribo-regulators that control the expression of the genes *lmo0919* and *lmo1652*, both encoding ABC transporter genes of unknown function (Figs. 4C-D). Whereas the alteration in the open/closed state of *lmo0919* by *rli53* was highly specific to lincomycin, *rli59* was more permissive and responded to several different translation inhibiting antibiotics (Figs. 4C and G). In *E. faecalis,* it was previously shown that expression of the *msrC* macrolide-resistance efflux pump increases in response to erythromycin exposure (40). Our data suggest that the *msrC* response results from a coordinated activity of its promoter and a novel termination-based regulator, which, upon exposure to the antibiotic, act in concert to increase both the transcription initiation rate (7.3 fold) and read-through into the gene (4.6 fold)(Figs 4E, 4G). Interestingly, we detected a similar promoter-termination synchronized activity for the *B. subtilis vmlR* gene (Fig. 4B). Finally, we found an additional lincomycin-specific termination-based regulator that controls the expression of yet another ABC transporter of unknown function, *EF2720*, in *E. faecalis* (Fig. 4F).

The presence of antibiotic-responsive, termination-based regulatory elements upstream of specific genes in *L. monocytogenes* and *E. faecalis* suggest that these are possible novel antibiotic resistance genes. We further characterized the antibiotic-based regulation of *lmo0919*, an ABC transporter of unknown function in *L. monocytogenes*. This gene was previously suggested to be involved in antibiotic resistance based on its distant homology to the staphylococcal Vga gene and its heterologous activity in staphylococcal hosts (41), but its function in *L. monocytogenes* remained unknown. Remarkably, we found that deletion of *lmo0919* rendered *L. monocytogenes* 4-fold more sensitive to the antibiotic lincomycin, but did not reduce the MIC of other antibiotic classes (table S7). The protein encoded by *lmo0919* therefore confers lincomycin-specific antibiotic resistance, consistent with the specific activation of its 5'UTR regulator by lincomycin but not by erythromycin or chloramphenicol (Figs. 4D, 4G).

The mechanism of antibiotics-mediated conditional termination in *lmo0919*

Inspection of the regulatory 5' UTR sequence of *lmo0919* revealed a potential two-stem, terminator/antiterminator structure (Fig. 5A). Such structures are common in riboswitches and attenuators, and can adopt two alternative conformations, one that generates a transcriptional terminator (Fig. 5A, left) and another in which the anti-terminator promotes transcriptional read-through by interfering with terminator formation (Fig. 5A, right). To enquire whether this mode of regulation occurs in the case of *lmo0919*, we engineered mutations in either the first or the second arm of the first stem, disrupting the putative anti-anti-terminator or the anti-terminator, respectively (Fig. 5B). Consistent with the model, deletion of 8 nucleotides from the anti-terminator kept the regulator in a constitutively "closed" state even in the presence of lincomycin antibiotic, rendering the bacteria sensitive (Figs. 5B-E and 5F; table S8). In contrast, deletion of 8 nucleotides from the anti-anti-terminator freed the anti-terminator to interfere with the terminator structure, leading to

constitutive read-through (“open” state) even in the absence of antibiotics, and resulting in increased resistance to lincomycin (Figs. 5B-E and 5G). These results support a model in which the lincomycin-dependent activation of *lmo0919* expression is mediated by a structural interplay of terminator/anti-terminator structures in the 5’UTR of this gene.

The structural alterations in the *lmo0919* ribo-regulator could either be mediated by direct binding of the antibiotic to the ribo-regulator (i.e., a riboswitch), or by attenuation, where the lincomycin-inhibited ribosomes stall on a uORF in the ribo-regulator, thus shifting the ribo-regulator structure from a “closed” to an “open” state (as suggested for the *bmrB* regulator in *B. subtilis* (30)). To differentiate between these mechanisms, we measured the lincomycin-dependent induction of *lmo0919* in *L. monocytogenes* expressing the ErmC 23S rRNA methyltransferase (23, 42). In these bacteria the ribosomes are di-methylated at position A2058 of the 23S rRNA, rendering the ribosomes resistant to lincomycin (42). Strikingly, in ErmC-expressing bacteria the *lmo0919* regulator was no longer responsive to lincomycin (fig. S6), suggesting that this ribo-regulator depends on stalled ribosomes for its activity and does not interact directly with the antibiotic molecule.

We then performed a comparative analysis of the 5’UTR sequences of *lmo0919* homologs in various Gram positive bacteria (23). While the nucleotide sequence of the ribo-regulator showed almost no conservation between species, the terminator/anti-terminator architecture was strictly conserved among all homologs (figs. S7, S8). Remarkably, despite the near lack of sequence conservation, all regulators contained a 3-amino-acid uORF exactly overlapping the inhibitory anti-anti-terminator sequence (Figs. 5B, S7, S8). Although such small ORFs were never previously reported to be involved in transcriptional attenuation, the strong positional conservation of the uORF in the ribo-regulator led to the hypothesis that its translation forms the basis for the attenuation-based regulation. Indeed, a GFP fusion assay showed that this uORF is translated in *L. monocytogenes in-vivo* (fig. S9) (23).

To characterize the effects of lincomycin on the interaction between the ribo-regulator and the ribosome we measured the levels of ribosome occupancy over the ribo-regulator in control and lincomycin-treated bacteria using ribosome profiling (Ribo-seq) (23, 43). Strikingly, we detected ~5 and ~2 fold increase in ribosome occupancy over the 3aa uORFs in *L. monocytogenes* and *L. innocua*, respectively, following brief exposure to lincomycin (fig. S10) (23). These results show that lincomycin-inhibited ribosomes specifically stall at the 3aa uORF that overlaps the anti-anti-terminator sequence.

Collectively, these results point to an attenuation-based regulatory mechanism where the association of the ribosome with the antibiotic leads the ribosome to stall on a nine base uORF that overlaps the anti-anti-terminator, releasing the anti-terminator to interfere with terminator folding, and thus allowing read-through into the antibiotic resistance gene. Indeed, a single-base mutation that changed the ATG (Met) initiation codon of the uORF into ACG led to suppressed lincomycin dependent read-through, validating the model (Figs. 5B, 5D, 5H).

Notably, the *lmo0919* regulator is specifically activated by lincomycin but not by erythromycin (Fig 4), although both antibiotics induce ribosome stalling. While antibiotics

of the lincomycin family inhibit ribosome progression after the incorporation of 1-2 amino acids, erythromycin requires the addition of 6-8 amino acids to the nascent chain before it stalls the ribosome (44). It is therefore possible that the specificity of the *lmo0919* ribo-regulator to lincomycin stems from the short size of its functional uORF.

Abundance of antibiotic dependent ribo-regulation in the human microbiome

The presence of multiple antibiotic-responsive, termination-based regulatory elements in three evolutionary distant bacterial species prompted us to hypothesize that this mode of regulation is commonly controlling antibiotic resistance in nature. We thus probed for such regulatory elements in the human oral microbiome, a complex microbial community comprised of hundreds of commensal teeth- and mouth-associated bacterial species that are frequently naturally exposed to antibiotics (45).

We used a meta-transcriptomics approach (denoted here *meta-term-seq*) in order to probe the transcriptional profile of the microbial consortium in a single experiment. For this, teeth-associated bacteria were sampled from three healthy individuals and were pooled in tubes containing BHI medium with and without the antibiotic lincomycin for 15 minutes. We applied term-seq and RNA-seq on pooled RNA, and mapped RNA reads to the >400 reference genomes from the human oral microbiome project (23, 45, 46). We further studied the antibiotic-responsive meta-term-seq profiles in the 167 species that showed significant expression of at least 10% of their genes (23).

Remarkably, operons activated by alleviation of premature termination in response to lincomycin were abundantly found in members of the human oral microbiome. We detected 21 regulatory elements, overall controlling 57 genes, in which transcriptional read-through was significantly increased following the application of lincomycin (Figs. 6, S11; tables S1, S8) (23). Such elements were detected in 21% (13/61) of the Firmicutes studied, indicating that this mode of regulation is common in bacteria in this phylum. The genes regulated by the antibiotic-responsive *cis*-acting RNA elements included several different classes of multidrug antibiotics exporters and efflux pumps (47, 48), rRNA methylases known to confer antibiotic resistance via modification of the ribosomal RNA (39), acetyltransferases known to directly deactivate the antibiotic via acetylation (49), genes annotated as tetracycline resistance small-GTPases that rescue antibiotic-bound ribosomes (50), and additional genes that have no described antibiotic resistance (Figs. 6, S11; tables S1, S8). These results highlight meta-term-seq as a method to probe gene regulation in microbial consortia, and reveal a common control mechanism for antibiotic-resistance genes in human-associated bacteria.

Discussion

We present here an unbiased experimental method for high-throughput discovery of conditional-termination-based regulators in individual bacteria as well as in microbiomes. Moreover, we developed a screening procedure that measures the *in-vivo* read-through levels of every regulator in the genome in parallel, thus enabling the identification of regulators

that specifically respond to a given metabolite. By screening for ribo-regulators that respond to antibiotic molecules, we highlight a common form of regulation of antibiotics-resistance genes, and expose the molecular details entailing its mechanism of action.

Through the use of term-seq, which does not rely on comparative genomics, we overcome the challenge of identifying highly divergent or evolutionarily new regulators, as well as short regulators, both of which are generally challenging or even impossible to find when relying on sequence conservation (19). Furthermore, with the ability of term-seq to measure the *in-vivo* activity of every expressed regulator in the cell in parallel we prevent experimental biases that stem from artificial transfer of the regulator to a model organism, and allow for large scale screens/studies of regulators in organisms lacking genetic-engineering tools. In addition, our meta-term-seq approach enables parallel discovery of ribo-regulators in multiple organisms belonging to a bacterial consortium, even if these organisms are non-cultivated. Nevertheless, while our approach identifies metabolite-responsive regulators, it does not differentiate between riboswitches, attenuators and protein-dependent termination, and moreover cannot identify riboswitches and attenuators functioning via translation inhibition rather than premature termination. Our approach will also work only for metabolites that can enter the cell (for direct binding to riboswitches) or can be sensed by the cell. Finally, another limitation of the approach is that the read-through response we record in the regulator may be due to a metabolite different than the one added in the screen. This would occur, for example, when the added metabolite leads to changes in the levels of the true metabolite. However, since the riboswitch-mediated response is direct and hence expected to be very rapid, these secondary effects could be mitigated if the exposure to the screened-for metabolite is very short, as done in our antibiotic-exposure experiments.

Termination-based regulation of antibiotic resistance genes have so far been sporadically described (30, 32, 39). Our identification of numerous regulators in model organisms and in many species of the human oral microbiome indicates that such regulation of antibiotic resistance genes is very common in gram positive bacteria. Moreover, even in the three model organisms that we studied in depth, additional antibiotic-dependent regulators may be present. For example, in *B. subtilis* we identified a novel regulator upstream to *BSU39010* (Fig. 2E). This gene is predicted to methylate the 23S rRNA at position G748, which was shown to provide a highly specific resistance to the macrolide antibiotic tylosin, but not to other macrolides, in *Streptomyces fradiae* (51). Although we did not observe an antibiotic-dependent response in this regulator, it is conceivable that it would show a specific response to tylosin, which was not included in our screen. In addition, regulators were found for the *L. monocytogenes lmo2760* and the *E. faecalis EF0660* genes (Fig. 2H), both of which are homologous to multidrug efflux pumps. These regulators possibly respond to antibiotics other than the ones we used in our screen.

The importance of termination-based *cis*-regulators in maintaining the versatile physiology of bacteria is evident from their nearly ubiquitous distribution cross the bacterial kingdom (33). We now provide the tools with which we can identify and characterize many of these in the future.

Materials and Methods

Oligonucleotides, wild-type bacterial strains and culture conditions

All oligonucleotides used in this study were purchased from Sigma or Integrated DNA Technologies (IDT, San Jose, California) (table S9). *Bacillus subtilis* str. 168, *Listeria monocytogenes* EGDe, *Listeria innocua* Clip11262 and *Enterococcus faecalis* ATCC 29212 were cultured under aerobic conditions at 37°C with shaking in either LB (10g/L tryptone, 5g/L yeast extract 5g/L NaCl), TB (12g/L tryptone, 24g/L yeast extract, 0.4% glycerol, 2.2g/L KH_2PO_4 and 9.4g/L K_2HPO_4), Brain Heart Infusion (BHI) broth (Difco, Franklin Lakes, New Jersey), or M9 minimal media (0.5% w/v glucose, 2 g/L $[NH4]_2$ SO_4, 18.3 g/L K2 HPO_4 $\cdot 3H_2O$, 6 g/L $KH2PO_4$, 1 g/L sodium citrate, 0.2 g/L $MgSO_4$ $\cdot 7H_2O$, 5μM $MnCl_2$, and 5μM $CaCl_2$, tryptophan (Sigma, St. Louis, Missouri) 50μg/mL).

Lysine responsive regulation

B. subtilis was grown overnight in LB and then diluted 1:200 into 150ml of M9 media supplemented with lysine and methionine (50μg/mL each). Bacteria were grown to OD_{600} = 0.9-1.0, washed, and then resuspended to an OD_{600} = 0.3 in 3ml of M9 media, containing the following combinations of amino acids at a final concentration of 50μg/mL: lysine and methionine (lys+ met+), methionine only (lys- met+), or lysine only (lys+ met-). Cells were incubated for 2h and collected by centrifugation (4000 rpm, 5min, and 4°C) followed by flash freezing. Samples were stored in -80°C until RNA extraction.

Antibiotics responsive regulators

A sublethal concentration for the antibiotics lincomycin, erythromycin, chloramphenicol, kanamycin, ofloxacin, ampicilin and bacitracin (Sigma) was determined for each of the organisms used in this study as follows. Bacterial cultures were propagated in LB or BHI overnight in triplicates and diluted 1:200 into fresh media. Cultures were grown to early exponential phase (OD_{600} = 0.1-0.2) and then supplemented with serially diluted antibiotics stocks. The growth rate was dynamically monitored in intervals of 10-15min using a 96 well plate format OD reader (Infinite M200 Tecan) for a period of at least 4 hours. The highest antibiotics concentration that did not cause growth-rate inhibition as compared to the no-antibiotics control was chosen as the sublethal dosage (Table S7). To identify antibiotic-responsive regulators, bacteria were grown in LB or BHI in triplicates as described above and, upon reaching early exponential phase, 5ml cultures were independently exposed for 15 minutes to the sublethal concentration of each antibiotic as determined above. Bacteria were then collected by centrifugation, flash frozen and stored in -80°C until RNA extraction.

RNA isolation

Frozen bacterial pellets were lysed using the Fastprep homogenizer (MP Biomedicals, Santa Ana, California) and RNA was extracted with the FastRNA PRO™ blue kit (MP Biomedicals, 116025050) according to the manufacturer's instructions. RNA levels and integrity were determined by Qubit® RNA BR Assay Kit (Life technologies, Carlsbad, California, Q10210) and Tapestation (Agilent, Santa Clara, California, 5067-5576),

Europe PMC Funders Author Manuscripts

respectively. All RNA samples were treated with TURBO™ DNase (Life technologies, AM2238).

Construction of mutated *Listeria* strains

For mutant generation with pMAD-based plasmids (52), ~600nt regions of complementarity both upstream and downstream of a targeted region were either ordered as gBlocks (IDT) and amplified with gBlock-Up and Down oligonucleotides (table S9) complimentary to uniform flanks on each gBlock corresponding to the 40 nts on either side of the pMAD multi-cloning site, or PCR amplified with Phusion High fidelity polymerase and reagents (Finnzymes, F-553) using genomic DNA as a template and then joined by a second splice overlap extension PCR reaction using the first two PCR products as template to generate a Upstream-Downstream (UD) PCR product (table S9, *lmo0919* deletion). PCR products were subsequently purified with QIAquick PCR purification columns (Qiagen, Hilden, Germany, 28104), digested with the SalI and XmaI restriction enzymes (New England BioLabs, NEB, Ipswich, Massachusetts), purified again as before, and ligated into SalI/XmaI digested pMAD plasmid for 1 hr at 25°C with T4 DNA ligase (NEB, M0202S). 2μl of each ligation were transformed into chemically competent *E. coli* Top10 (Invitrogen, Carlsbad, California, C404003) cells according to the manufacturer's instructions. Transformants were screened by PCR and Sanger sequencing for the presence of the appropriate insert. Electrocompetent *L. monocytogenes* strains were transformed with the respective plasmid and mutagenesis carried out as described previously (52). Briefly, after transformation and plating onto selective BHI, 5ug/ml erythromycin (Em) 80ug/ml 5-bromo-4-chloro-3-indolyl-β-D-galactopyranoside (X-gal) plates, bacteria were grown at 30°C for two days. A single blue colony was picked and transferred to liquid BHI broth and grown for an additional 6hrs at 30°C. The colony was then diluted 1:1000 into 10ml of BHI-Em and grown overnight at 42°C, which prevents pMAD replication in the cytosol owing to a temperature sensitive ori. Serial dilutions were plated onto BHI-X-gal-Em plates and grown for two days at 42°C, and the process was reiterated several times until white colonies, in which the plasmid integrated into the genome, were recovered. Colonies were screened by colony PCR, and mutants were confirmed by Sanger sequencing.

For the construction of the GFP reporter strain, a translational fusion was constructed by generating a synthetic 1936bp fragment (*rli53*-GFP) encompassing the upstream region of *rli53* (591bp), the 5' of rli53 (40bp) and a small spacer (30nt) fused to the Green Fluorescent protein optimized for Listeria (53) that lacks the initiator codon and followed by the downstream region of *rli53* (549bp) (IDT, table S9). The construction was cloned into the BamHI and EcoRI restriction sites of the suicide vector pMAD (52) to generate the plasmid pMAD-rli53-GFP used to transform the wild-type strain *L. monocytogenes* EGD-e as described above, and generating the *L. monocytogenes* strain expressing the chromosomic fusion *rli53*-GFP. The sequence was verified by DNA sequencing using oligonucleotides (*lmo0918*-upstream and *lmo0919*-downstream, table S9).

Minimal Inhibitory Concentration (MIC) determination

The MIC was determined in broth culturing conditions in the presence of serially diluted antibiotic concentrations. Briefly, the bacterial strains were grown overnight at 37°C in BHI

agarose plates and 1-3 single colonies were collected into 1ml of BHI broth. The OD_{600} was adjusted to 0.01 and then diluted 1:10 into a 96-well plate containing a final volume of 200µl BHI supplemented with two-fold serial dilutions of lincomycin, erythromycin and chloramphenicol. The samples were grown over two days at 37°C without shaking and the MIC was determined as the lowest antibiotic concentration to fully inhibit growth.

Term-seq library preparation

DNAse treated RNA (1-5µg) was subjected to a 3' end specific ligation by mixing 5µl RNA solution with 1µl of a 150µM DNA adapter solution (table S9), 2.5µl 10X T4 RNA ligase1 buffer, 2.5µl 10mM ATP, 2µl DMSO, 9.5µl 50% PEG8000 and 2.5µl T4 RNA ligase1 enzyme (NEB, M0204). The reaction was incubated for 2.5h at 23°C and then cleaned by adding 2.2x (55µl) paramagnetic SPRI beads (Agencourt AMPure XP, Beckman Coulter, Brea, California), mixing well by pipetting and leaving the reaction-bead solution to rest at room temperature for 2min. The supernatant was separated from the beads using a 96-well magnetic separator (Invitrogen). Beads were washed on magnet (beads securely attached) by discarding the solution and adding 120µl 70% ethanol (EtOH), allowing an incubation period of 1min. The cleanup stage was repeated and the beads were air dried for 5min. The RNA was eluted in 5-10µl H_2O. The RNA was fragmented with fragmentation buffer (Ambion) in 72°C for 1.5min. The fragmentation reaction was cleaned using SPRI beads 2.2x as described above, and eluted in 28µl H_2O. Ribosomal RNA was depleted using the Ribo-Zero™ rRNA Removal Kit (epicenter, MRZB12424) or MICROBExpress™ (Life technologies, AM1905) according to the manufacturer's instructions. Depleted RNA was reverse transcribed by incubating 11µl of RNA with 1µl of 10µM reverse transcription primer (table S9), incubating at 65°C for 5min and immediately placing on ice for 2min. 2µl AffinityScript reverse transcriptase (Agilent, 600559), 2µl 10X Affinity Script Buffer, 2µl 100mM DTT and 2µl 10mM dNTPs (Sigma, D7295) were added, and the reaction was incubated at 42°C for 45min and then terminated by incubation at 75°C for 15min. To degrade the RNA template, 1µl of RNase H (NEB, M0297) was added and the reaction was incubated for an additional 30min at 37°C. The reaction was cleaned by using SPRI beads at a 2.2x ratio (46µl) and eluted in 5.5µl H_2O. 5µl of the resulting cDNA was subjected to a second 3' end ligation, as above, but using a cDNA specific ligation adapter (table S9). The reaction was incubated at 23°C for 4-8h and then cleaned with SPRI beads at a 1.8x ratio (45µl), eluting the cDNA in 23µl H_2O. 22µl of ligated cDNA solution was mixed with 1.5µl of forward and reverse primers, at 25µM each (table S9) and 25µl KAPA Hi-Fi PCR ready mix (KAPA Biosystems, Wilmington, Massachusetts, KK2601). Library was amplified using the manufacturer's protocol with 16-18 amplification cycles. The final term-seq library was cleaned with SPRI beads at a 0.9x ratio (45µl) and the concentration and size distribution were determined by Qubit® dsDNA BR Assay Kit (Life technologies, Q32850) and the dsDNA D1000 Tapestation kit (Agilent, 5067-5582), respectively.

RNA-seq and 5' end sequencing

For RNA-seq library preparation, 4µg DNase treated RNA was fragmented in 20µL reaction volume as described above and cleaned by adding 2.5x (50µl) SPRI beads and 30% v/v Isopropanol (30µl). The beads were washed with 120µl 80% EtOH and then air dried as described above. The RNA was eluted in 26µl H_2O and ribosomal RNA was depleted as in

term-seq. Strand specific RNA-seq was performed with the NEBNext® Ultra™ Directional RNA Library Prep Kit (NEB, E7420) with the following adjustments to the manufacturer's instructions: All cleaning steps were carried out with 2.5x SPRI beads and 30% v/v isopropanol combinations, the washing steps were performed with 450µl 80% EtOH, and only one cleanup step was performed after the end repair step. The resulting libraries concentrations and sizes were evaluated as in term-seq. For 5'end sequencing, the RNA was divided into a Tobacco Acid Pyrophosphatase (TAP) treated and untreated (noTAP) reactions which were subsequently sequenced using a 5' end specific library preparation protocol described in *Wurtzel et al* (25). In *B. subtilis*, the 5' end libraries were prepared with bacteria grown to early exponential phase in TB medium. For *L. monocytogenes*, 5' end data was taken from *Wurtzel et al* (25).

Deep-sequencing, read mapping and counting

RNA-seq, 5'end and term-seq libraries generated in this study (table S10) were sequenced using the Illumina Miseq, Hiseq1500 or NextSeq500 platforms. Sequenced reads were demultiplexed and adapters were trimmed using Casava v1.8.2. Reads were mapped to the reference genomes (Gene annotation and sequences were downloaded from Genbank: AL009126, NC_003210, NC_003212 NC_004668 for *Bacillus subtilis* str. 168, *Listeria monocytogenes* EGD-e, *Listeria innocua* Clip11262 and *Enterococcus faecalis* V583, respectively) using NovoAlign (Novocraft) V3.02.02 with default parameters, discarding reads that were non-uniquely mapped as previously described in *Wurtzel et al* (25). All downstream analyses were performed using custom written perl and R scripts (available through GitHub under repository aad9822).

RNA-seq-mapped reads were used to generate genome-wide RNA-seq coverage maps. 5'end and term-seq positions were determined as the first nucleotide position of the mapped read. Total 5'end or term-seq coverage was calculated per nucleotide position in the genome. The data was visualized using a custom browser as described in *Wurtzel et al* (25) (Figs. 1-5). TSSs were determined as in *Wurtzel et al* (25). Briefly, the ratio between TAP-treated (TAP) and untreated (noTAP) was calculated for each genomic position covered by least 4 reads in the TAP condition. The maximal 5'UTR allowed was set to 450nt and the TSS was chosen as the site with a TAP/noTAP ratio greater than 2 for *B. subtilis* and greater than 1 for *L. monocytogenes* and *E. faecalis*. In cases where multiple potential TSSs were available, the site with the highest coverage was chosen as the gene TSS.

Terminator identification and analysis

For the assignment of terminators to genes, the downstream sequence of each gene (up to 150nt, allowing up to 10nt invasion to the next gene) was scanned for term-seq sites that were covered by a minimum of 4 reads in each of the three biological replicates. In case multiple sites were observed, the site with the highest coverage was selected as the terminator. This filtering resulted in 84.4% (+/- 0.7%) of the reads mapping to non-coding positions, representing >50 fold enrichment over what would have been expected by chance based on the coding:non-coding composition of the *B. subtilis* genome (p=0, binomial exact test). For terminator sequence and structure analysis, the 40nt upstream and 20nt downstream sequences were collected for each terminator and folded *in-silico* via the

RNAfold software using the standard parameters (54). For 96% (1382/1443) of the sites we predicted as terminators there was a clear stem/loop structure preceding the site, with 91% (1302/1443) of them preceded by at least 4 uridine residues in the eight bases immediately upstream to the termination position, in agreement with the known features of Rho-independent terminators (table S2; fig. S1). Nucleotide logos were generated using WebLogo (55)

Previously established terminators inferred by experimental assays such as northern blots or S1 nuclease mapping of the 3' end (56) were collected for *B. subtilis* genes covered by at least 25 RPKM RNA-seq reads (table S11) and then compared to the term-seq inferred terminator set described in table S1. We were able to detect 43 of 46 (93%) known, high-confidence terminators (table S11). Two of the three terminators that were not detected by term-seq were associated with genes of relatively low expression (76 and 90 reads per million per kilo-base) which could explain why they did not appear with a sufficient number of reads in the three biological repeats to be considered by our filtering criteria.

Discovery of premature termination

For the discovery of premature termination, the 5'UTR (the beginning of which was defined by the TSS) of each gene was scanned for term-seq sites that were covered by a minimum of 2 reads in each of the three biological replicates. Since the average length of a terminator is approximately 20-25nt (56), only 5'UTRs where the distance between the TSS and the term-seq site was at least 70nt were considered. Candidate regulators that displayed high term-seq density also across the gene body were discarded as likely degraded transcripts. In addition, candidates in which a potential secondary TSSs could be detected downstream of the premature terminator were discarded. Due to specific regulator degradation/processing patterns, a handful of premature terminator sites were manually corrected to a nearby, less covered term-seq site, if that site presented a stem-loop and polyU signature (corrections noted in Table S2). To differentiate between known and novel regulators, all candidate elements were compared against the Rfam database (33) (Rfam 11.0 2012-07-19: AL009126.3, AL591824.1 and AE016830.1 for *B. subtilis*, *L. monocytogenes* and *E. faecalis*, respectively) and the literature. All identified candidate regulators were independently compared to the online Rfam db.

Transcriptional read-through estimation using RNA-seq and term-seq

Term-seq average coverage across triplicates was calculated for the premature termination site and the full length gene termination site with a span of 10nt surrounding each terminator, and the fraction of full length (gene) terminations out of all termination events was used to as a measure of the transcriptional read-through (Fig. 3A). In cases where the regulator controlled the transcription of a multi-gene operon, which contained internal TSSs in addition to the primary one, RNA-seq was used to determine read-through in the first gene (Figs. 4C and 4F). RNA-seq coverage was used to measure the average read coverage over either the regulatory element or the gene, and the ratio between the two (gene-coverage divided by regulator-coverage) was used as an estimate for the short/long transcript ratio generated by regulator activity (Fig. 3A).

Europe PMC Funders Author Manuscripts

Term-seq analysis of *in-vitro* transcribed RNA

Term-seq libraries were prepared as above using *L. monocytogenes* RNA spiked in with 1µl 1:10 diluted ERCC RNA Spike-In Mix (Ambion, 4456740). Sequencing reads were mapped to the reference ERCC sequences and the number of term-seq reads mapped to the exact spike-in RNA 3' ends were counted and compared to the known RNA concentrations (fig. S2). Only Spike-in RNAs with a known concentration of at least 1 attmoles and that were covered by at least 1 term-seq read (n=58) were used in the analysis.

Ribosome immunization ErmC 23S methylation

L. monocytogenes EGDe pAT18-cGFP (53) was grown overnight in BHI media and then diluted 1:200 into fresh BHI. ErmC expression was induced by incubating the cultures with 0.5µg/ml erythromycin for 2h. The induced and the control (non-induced) samples were then exposed to 0.25µg/ml lincomycin or water as a control and incubated for 15min. Bacteria were harvested by centrifugation, flash-frozen, and the RNA was extracted, sequenced and analyzed as described above.

Comparative sequence analysis of *lmo0919* homologues

The Lmo0919 protein sequence was used to collect homologues in several Gram positive bacteria (fig. S7). 5'UTRs were estimated as the 275nt upstream top the homologous gene and were analyzed by multiple sequence alignment and *in-silico* RNA folding with Muscle (57) and with RNAfold (54), respectively. The upstream intergenic regions of *lmo0919* homologues identified in *Bacillus subtilis* subsp. *subtilis* str. 168, *Streptococcus gordonii* str. Challis substr. CH, *Enterococcus faecalis* V583, *Staphylococcus aureus* plasmid pVGA and *Clostridium botulinum* CDC54075 were collected using the Integrated Microbial Genomes database (IMG) (58) using the following IMG gene IDs 646317030, 640912864, 637415867, 643661871 and 2569227938, respectively.

Epifluorescence analysis

A colony of wildtype EGD-e and one of EGDe-rli53-GFP mutant *Listeria* were resuspended in 20µL of PBS and mounted on glass coverslips sealed with varnish. Samples were analyzed with an Axio Observer Z1 microscope (Zeiss) equipped with a spinning disk and an EvolveTM 512 EMCCD Camera (Photometrics). Images were acquired with an x100 oil immersion objective and processed with MetaMorph (Universal Imaging) and Icy (Pasteur Institute).

Ribosome profiling (Ribo-seq)

L. monocytogenes EGDe and *L. innocua* Clip11262 were grown overnight in BHI media and then diluted 1:200 into fresh 200ml BHI cultures. Cultures were grown to OD_{600} = 0.4-5 and then treated with either 0.5ug/ml lincomycin or water as a control for 15min. The bacteria were collected via the rapid-filtration method (43) and flash frozen in liquid-nitrogen. 650µl lysis buffer containing: 20 mM Tris 8.0, 10 mM MgCl2, 100 mM NH4Cl, 0.4% Triton X100, 0.1% NP-40, 1 mM chloramphenicol and 100 U/ml DNase I (NEB, M0303), were dropped over liquid nitrogen and added to the pellets. Frozen cell pellets were pulverized in the MM301 Mixer mill (Retsch, Haan, Germany) using 10ml stainless steel

grinding jar and 12mm grinding ball (Retsch), for 5 cycles, each at 30 Hz for 2 min and chilled in liquid nitrogen between cycles. Frozen lysates were thawed on ice for 20min and then centrifuged at 14,000rpm for 10min at 4°C and the supernatant was collected. MNase digestion was performed by mixing 1mg RNA with $CaCl_2$ (5mM final), 6µl Superase-In (Ambion) and 1.7µl MNase (NEB, M0247). The reaction was incubated for 1h in 25°C with shaking and terminated by adding 5mM EGTA (Sigma) and placing on ice. Monosomes were isolated by ultracentrifugation (Sw41 rotor, 35,000rpm for 2.5h at 4°C) of the samples over 10%-50% sucrose density gradient. Ribosomal footprints were collected as described in G.W. *Li et al* 2012 (43). Sequencing libraries were constructed using NEBNext® Small RNA Library Prep Set for Illumina® (NEB, E7330) according to the manufacturer's instructions. The sequencing reads were adapter trimmed using the FASTX-Toolkit (fastx_clipper -Q33 -a AGATCGGAAGAGCACACGTCTGAACTCCAGTCAC -l 25 -c -n -v -i input_fastq_file) and inserts sized 25nt to 40nt were aligned to reference genome and analyzed as above.

For each ribosome profiling sample we also sequenced the total RNA as following: 5µg total RNA was fragmented as above for 5min and then cleaned with SPRI as above and eluted in 16µl RNase free H_2O. The fragmented RNA was end-repaired using T4-polynucletide kinase (T4-PNK; NEB, M0201) by adding 2µl T4-PNK 10X buffer, 2 µl T4-PNK and then incubating the reaction at 37°C for 2h. The enzyme was deactivated by incubating the sample at 75°C for 15min and the RNA was collected by isopropanol precipitation. The resulting RNA was rRNA depleted as above and libraries were prepared with the NEBNext® Small RNA Library Prep Set for Illumina® (NEB, E7330) kit as above.

Meta-term-seq

Oral plaque was collected from three healthy individuals using a toothpick and then mixed into 1ml of liquid BHI media, pre-warmed to 37°C. The samples were vortexed for 10 seconds and then divided into tubes either containing BHI (control) or BHI supplemented with 1 µg/ml lincomycin, and then incubated with shaking at 37°C for 15 minutes. Bacteria were pelleted via centrifugation and were then flash-frozen. RNA extraction and library construction were done as described above. Sequencing reads were mapped to all contigs larger than 2.5kb taken from the 462 annotated genomes available at the Human Oral Microbiome Database (HOMD) (46). In cases where multiple closely related strains of a single species were present in the database, only one representative genome was selected. Only bacterial genomes in which at least 10% of all protein-coding genes were covered by 10 or more uniquely mapped reads were selected for further analysis. Sequencing reads were re-mapped to the final database of 167 bacterial genomes. Term-seq and 5' end sequencing reads were mapped using the novoalign –r Random option. To identify lincomycin responsive regulators, genes with a mapped TSS, premature term-seq site, and that were covered by >=50 RNA-seq reads and showed a >2.5 folds increase in expression in the lincomycin condition, were selected for read-through calculation. Candidate regulators were classified as lincomycin responsive if they increased their read-through by at least 2.5 folds following exposure to lincomycin, and that had a read-through greater than 10% in the lincomycin condition.

Construction of the phylogenetic tree in Fig. 6B was performed using 16S rRNA sequences, taken from the HOMD or from NCBI, and using the *phylogeny.fr* web-server with default parameters (59). The phylogenetic tree was deposited in the treebase online database (*treebase.org*) under accession number 18921.

Supplementary Material

Refer to Web version on PubMed Central for supplementary material.

Acknowledgements

We thank O. Wurtzel, I. Karunker, S. Doron, G. Amitai, G. Ofir, A. Millman, Y. Voichek, S. Melamed and R. Nir-Paz for insightful discussion. R.S. was supported, in part, by the ISF (personal grant 1303/12 and I-CORE grant 1796/12), the ERC-StG program (grant 260432), HFSP (grant RGP0011/2013 to R.S. and P.C), the Abisch-Frenkel foundation, the Pasteur-Weizmann council grant (to R.S and P.C), the Minerva Foundation, the Leona M. and Harry B. Helmsley Charitable Trust, and by a DIP grant from the Deutsche Forschungsgemeinschaft. P.C was supported by an ERC-AdV grant (BacCellEpi, #670823). Reference IRB for the microbiome analysis is 0315-15-HMO. Sequencing data was deposited in the European Nucleotide Database (ENA), accession PRJEB12568.

References

1. Winkler W, Nahvi A, Breaker RR. Thiamine derivatives bind messenger RNAs directly to regulate bacterial gene expression. Nature. 2002; 419:952–956. [PubMed: 12410317]
2. Mandal M, Boese B, Barrick JE, Winkler WC, Breaker RR. Riboswitches control fundamental biochemical pathways in Bacillus subtilis and other bacteria. Cell. 2003; 113:577–586. [PubMed: 12787499]
3. Sudarsan N, Wickiser JK, Nakamura S, Ebert MS, Breaker RR. An mRNA structure in bacteria that controls gene expression by binding lysine. Genes Dev. 2003; 17:2688–2697. [PubMed: 14597663]
4. Yanofsky C. Attenuation in the control of expression of bacterial operons. Nature. 1981; 289:751–758. [PubMed: 7007895]
5. Santangelo TJ, Artsimovitch I. Termination and antitermination: RNA polymerase runs a stop sign. Nat Rev Microbiol. 2011; 9:319–29. [PubMed: 21478900]
6. Dann CE, et al. Structure and mechanism of a metal-sensing regulatory RNA. Cell. 2007; 130:878–92. [PubMed: 17803910]
7. Winkler WC, Cohen-Chalamish S, Breaker RR. An mRNA structure that controls gene expression by binding FMN. Proc Natl Acad Sci U S A. 2002; 99:15908–13. [PubMed: 12456892]
8. Winkler WC, Nahvi A, Sudarsan N, Barrick JE, Breaker RR. An mRNA structure that controls gene expression by binding S-adenosylmethionine. Nat Struct Biol. 2003; 10:701–707. [PubMed: 12910260]
9. Sudarsan N, et al. Riboswitches in eubacteria sense the second messenger cyclic di-GMP. Science. 2008; 321:411–3. [PubMed: 18635805]
10. Irnov I, Winkler WC. A regulatory RNA required for antitermination of biofilm and capsular polysaccharide operons in Bacillales. Mol Microbiol. 2010; 76:559–75. [PubMed: 20374491]
11. Loh E, et al. A trans-acting riboswitch controls expression of the virulence regulator PrfA in Listeria monocytogenes. Cell. 2009; 139:770–9. [PubMed: 19914169]
12. Mellin JR, et al. Sequestration of a two-component response regulator by a riboswitch-regulated noncoding RNA. Science. 2014; 345:940–943. [PubMed: 25146292]
13. Paige JS, Nguyen-Duc T, Song W, Jaffrey SR. Fluorescence Imaging of Cellular Metabolites with RNA. Science. 2012; 335:1194–1194. [PubMed: 22403384]
14. Fowler CC, Brown ED, Li Y. Using a riboswitch sensor to examine coenzyme B12 metabolism and transport in E. coli. Chem Biol. 2010; 17:756–765. [PubMed: 20659688]
15. Isaacs FJ, Dwyer DJ, Collins JJ. RNA synthetic biology. Nat Biotechnol. 2006; 24:545–554. [PubMed: 16680139]

16. Benenson Y. Synthetic biology with RNA: Progress report. Curr Opin Chem Biol. 2012; 16:278–284. [PubMed: 22676891]
17. Blount KF, Breaker RR. Riboswitches as antibacterial drug targets. Nat Biotechnol. 2006; 24:1558–1564. [PubMed: 17160062]
18. Mulhbacher J, et al. Novel Riboswitch Ligand Analogs as Selective Inhibitors of Guanine-Related Metabolic Pathways. PLoS Pathog. 2010; 6:e1000865. [PubMed: 20421948]
19. Breaker RR. Prospects for riboswitch discovery and analysis. Mol Cell. 2011; 43:867–79. [PubMed: 21925376]
20. Weinberg Z, et al. Comparative genomics reveals 104 candidate structured RNAs from bacteria, archaea, and their metagenomes. Genome Biol. 2010; 11:R31. [PubMed: 20230605]
21. Sorek R, Cossart P. Prokaryotic transcriptomics: a new view on regulation, physiology and pathogenicity. Nat Rev Genet. 2010; 11:9–16. [PubMed: 19935729]
22. Güell M, Yus E, Lluch-Senar M, Serrano L. Bacterial transcriptomics: what is beyond the RNA horiz-ome? Nat Rev Microbiol. 2011; 9:658–69. [PubMed: 21836626]
23. Supplementary Materials and Methods, available as Online materials on the Science website.
24. Wurtzel O, et al. A single-base resolution map of an archaeal transcriptome. Genome Res. 2010; 20:133–41. [PubMed: 19884261]
25. Wurtzel O, et al. Comparative transcriptomics of pathogenic and non-pathogenic Listeria species. Mol Syst Biol. 2012; 8:583. [PubMed: 22617957]
26. Sarsero JP, Merino E, Yanofsky C. A Bacillus subtilis operon containing genes of unknown function senses tRNATrp charging and regulates expression of the genes of tryptophan biosynthesis. Proc Natl Acad Sci U S A. 2000; 97:2656–2661. [PubMed: 10706627]
27. Holmberg C, Rutberg L. An inverted repeat preceding the Bacillus subtilis glpD gene is a conditional terminator of transcription. Mol Microbiol. 1992; 6:2931–2938. [PubMed: 1479885]
28. Turner RJ, Lu Y, Switzer RL. Regulation of the Bacillus subtilis pyrimidine biosynthetic (pyr) gene cluster by an autogenous transcriptional attenuation mechanism. J Bacteriol. 1994; 176:3708–3722. [PubMed: 8206849]
29. Fujita Y. Carbon catabolite control of the metabolic network in Bacillus subtilis. Biosci Biotechnol Biochem. 2009; 73:245–259. [PubMed: 19202299]
30. Reilman E, Mars RT, van Dijl JM, Denham EL. The multidrug ABC transporter BmrC/BmrD of Bacillus subtilis is regulated via a ribosome-mediated transcriptional attenuation mechanism. Nucleic Acids Res. 2014; 42:11393–11407. [PubMed: 25217586]
31. Naville M, Gautheret D. Premature terminator analysis sheds light on a hidden world of bacterial transcriptional attenuation. Genome Biol. 2010; 11:R97. [PubMed: 20920266]
32. Ohki R, Tateno K, Takizawa T, Aiso T, Murata M. Transcriptional termination control of a novel ABC transporter gene involved in antibiotic resistance in Bacillus subtilis. J Bacteriol. 2005; 187:5946–5954. [PubMed: 16109936]
33. Nawrocki EP, et al. Rfam 12.0: updates to the RNA families database. Nucleic Acids Res. 2014; 43:D130–D137. [PubMed: 25392425]
34. de Noordhout CM, et al. The global burden of listeriosis: a systematic review and meta-analysis. Lancet Infect Dis. 2014; 14:1073–1082. [PubMed: 25241232]
35. Sava IG, Heikens E, Huebner J. Pathogenesis and immunity in enterococcal infections. Clin Microbiol Infect. 2010; 16:533–540. [PubMed: 20569264]
36. Toledo-Arana A, et al. The Listeria transcriptional landscape from saprophytism to virulence. Nature. 2009; 459:950–6. [PubMed: 19448609]
37. Mraheil MA, et al. The intracellular sRNA transcriptome of Listeria monocytogenes during growth in macrophages. Nucleic Acids Res. 2011; 39:4235–4248. [PubMed: 21278422]
38. Burke TP, et al. Listeria monocytogenes Is Resistant to Lysozyme through the Regulation, Not the Acquisition, of Cell Wall-Modifying Enzymes. J Bacteriol. 2014; 196:3756–3767. [PubMed: 25157076]
39. Kwak JH, Choi EC, Weisblum B. Transcriptional attenuation control of ermK, a macrolide-lincosamide-streptogramin B resistance determinant from Bacillus licheniformis. J Bacteriol. 1991; 173:4725–4735. [PubMed: 1713206]

40. Aakra Å, et al. Transcriptional Response of Enterococcus faecalis V583 to Erythromycin. Antimicrob Agents Chemother. 2005; 49:2246–2259. [PubMed: 15917518]
41. Chesneau O, Ligeret H, Hosan-Aghaie N, Morvan A, Dassa E. Molecular analysis of resistance to streptogramin A compounds conferred by the Vga proteins of staphylococci. Antimicrob Agents Chemother. 2005; 49:973–80. [PubMed: 15728891]
42. Wilson DN. The A-Z of bacterial translation inhibitors. Crit Rev Biochem Mol Biol. 2009; 44:393–433. [PubMed: 19929179]
43. Li GW, Oh E, Weissman JS. The anti-Shine-Dalgarno sequence drives translational pausing and codon choice in bacteria. Nature. 2012; 484:538–41. [PubMed: 22456704]
44. Tenson T, Lovmar M, Ehrenberg M. The Mechanism of Action of Macrolides, Lincosamides and Streptogramin B Reveals the Nascent Peptide Exit Path in the Ribosome. J Mol Biol. 2003; 330:1005–1014. [PubMed: 12860123]
45. Dewhirst FE, et al. The human oral microbiome. J Bacteriol. 2010; 192:5002–5017. [PubMed: 20656903]
46. Chen T, et al. The Human Oral Microbiome Database: a web accessible resource for investigating oral microbe taxonomic and genomic information. Database (Oxford). 2010; 2010:baq013. [PubMed: 20624719]
47. Méndez C, Salas J. The role of ABC transporters in antibiotic-producing organisms: drug secretion and resistance mechanisms. Res Microbiol. 2001; 152:341–350. [PubMed: 11421281]
48. Zhao Q, et al. Influence of the tonB energy-coupling protein on efflux-mediated multidrug resistance in Pseudomonas aeruginosa. Antimicrob Agents Chemother. 1998; 42:2225–2231. [PubMed: 9736539]
49. Davies J, Wright GD. Bacterial resistance to aminoglycoside antibiotics. Trends Microbiol. 1997; 5:234–240. [PubMed: 9211644]
50. Starosta AL, Lassak J, Jung K, Wilson DN. The bacterial translation stress response. FEMS Microbiol Rev. 2014; 38:1172–1201. [PubMed: 25135187]
51. Douthwaite S, Crain PF, Liu M, Poehlsgaard J. The tylosin-resistance methyltransferase RlmAII (TlrB) modifies the N-1 position of 23 S rRNA nucleotide G748. J Mol Biol. 2004; 337:1073–1077. [PubMed: 15046978]
52. Arnaud M, Chastanet A, Débarbouillé M. New vector for efficient allelic replacement in naturally nontransformable, low-GC-content, gram-positive bacteria. Appl Environ Microbiol. 2004; 70:6887–6891. pMAD. [PubMed: 15528558]
53. Balestrino D, et al. Single-cell techniques using chromosomally tagged fluorescent bacteria to study Listeria monocytogenes infection processes. Appl Environ Microbiol. 2010; 76:3625–3636. [PubMed: 20363781]
54. Lorenz R, et al. ViennaRNA Package 2.0. Algorithms Mol Biol. 2011; 6:26. [PubMed: 22115189]
55. Crooks GE, Hon G, Chandonia J-M, Brenner SE. WebLogo: a sequence logo generator. Genome Res. 2004; 14:1188–90. [PubMed: 15173120]
56. de Hoon MJL, Makita Y, Nakai K, Miyano S. Prediction of transcriptional terminators in Bacillus subtilis and related species. PLoS Comput Biol. 2005; 1:e25. [PubMed: 16110342]
57. Edgar RCC. MUSCLE: multiple sequence alignment with high accuracy and high throughput. Nucleic Acids Res. 2004; 32:1792–1797. [PubMed: 15034147]
58. Markowitz VM, et al. IMG: The integrated microbial genomes database and comparative analysis system. Nucleic Acids Res. 2012; 40:115–122.
59. Dereeper A, et al. Phylogeny.fr: robust phylogenetic analysis for the non-specialist. Nucleic Acids Res. 2008; 36doi: 10.1093/nar/gkn180

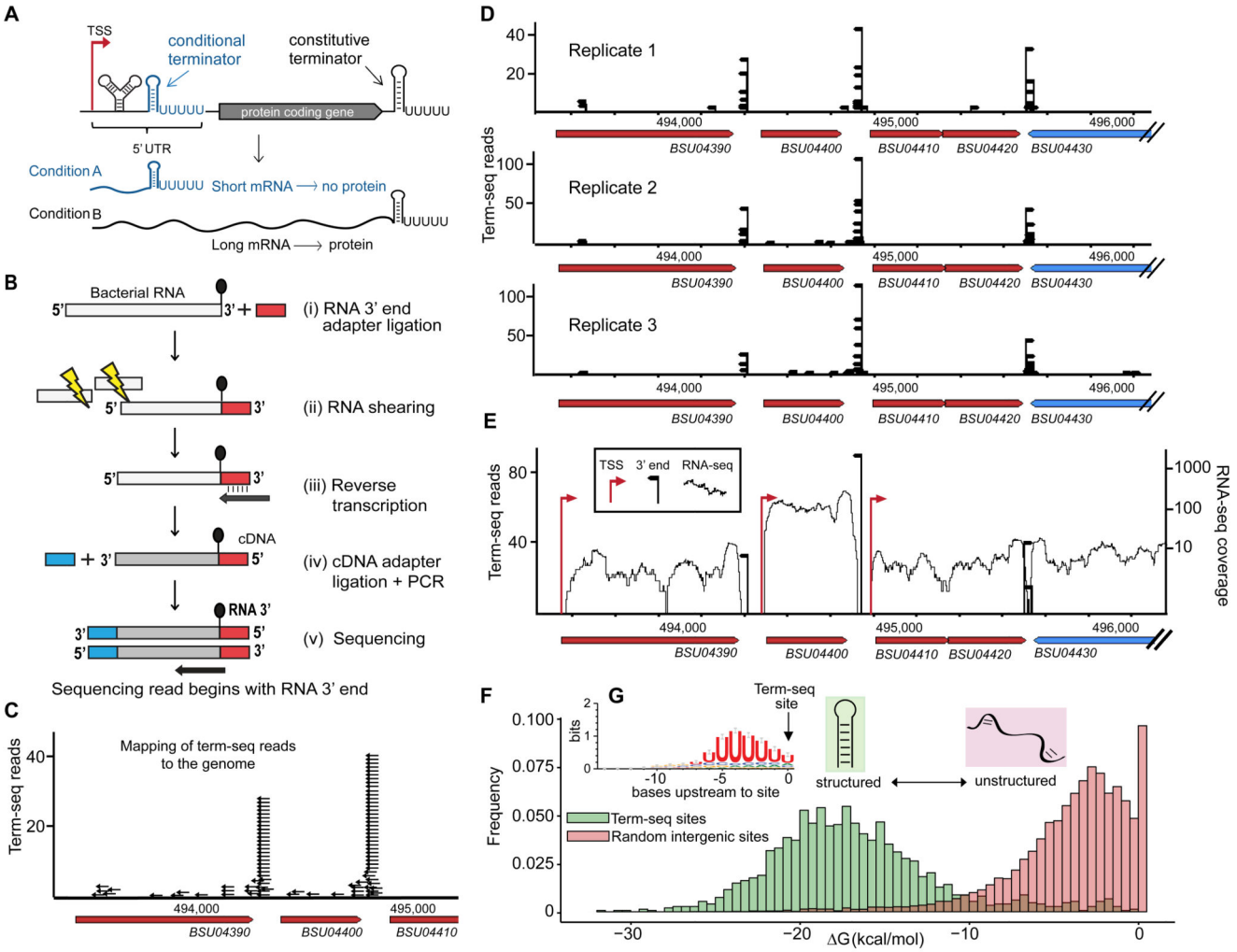

Fig. 1. Term-seq maps RNA termini across the genome.

(**A**) Regulation by conditional termination in bacteria. A model 5' UTR containing a ribo-regulator (riboswitch, protein-binding leader or attenuator) that differentially folds to generate a condition-specific premature terminator. (**B**) Schematic representation of the term-seq protocol. (**C**) Mapping of term-seq reads to the genome yields a typical pattern where the majority of reads map to discrete intergenic positions marking RNA 3' ends. Black arrows represent individual mapped reads. (**D**) Data from three biological replicates over a representative 3kb window of the *B. subtilis* genome show reproducibility. Black arrowheads represent positions supported by term-seq reads, with arrow height (y-axis) representing the number of reads supporting the position. (**E**) Multi-layered RNA sequencing data provides an integrative view of the bacterial transcriptome. Black arrowheads represent predicted term-seq termination sites, with arrow height indicating the average number of reads in three biological replicates. Black curve represents RNA-seq coverage. Red arrowheads mark the position of transcription start sites (TSSs), as inferred from transcriptome-wide sequencing of RNA 5' ends (23–25). (**F**) Folding energy of RNA

Europe PMC Funders Author Manuscripts

termini predicted by term-seq (n=1443, green bars) compared with random intergenic sites (n=10,000, red bars). (**G**) Uridine-rich tail upstream to term-seq sites (n=1443).

Europe PMC Funders Author Manuscripts

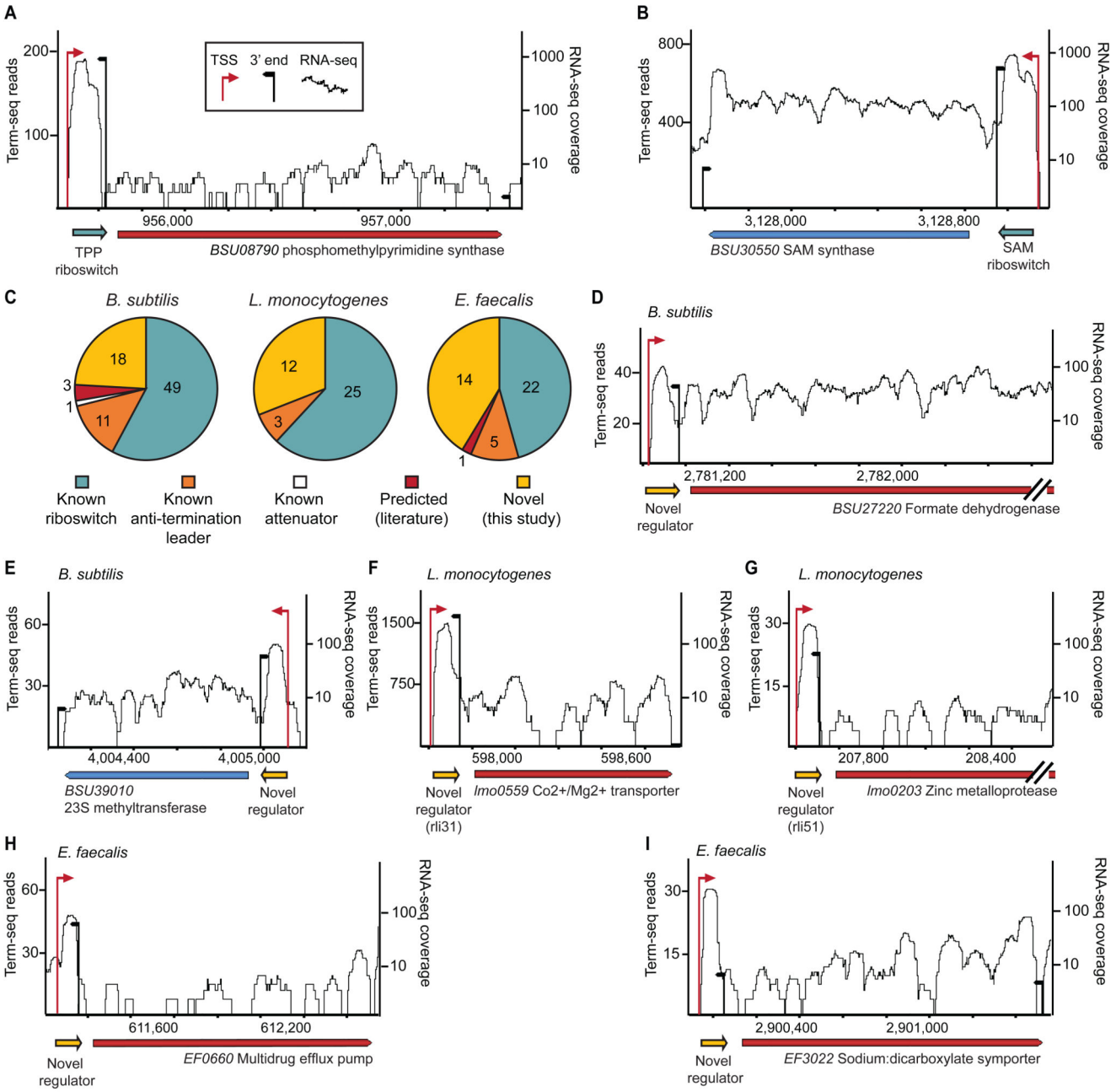

Fig. 2. Discovery of genes regulated by conditional termination.

Known riboswitches in *B. subtilis* display a typical pattern of premature termination in the 5'UTR. In both (**A**) Thiamine pyrophosphate (TPP) riboswitch and (**B**) Lysine riboswitch (cyan arrows) a term-seq site is observed downstream to the riboswitch. (**C**) Known and novel regulators identified by applying term-seq on *B. subtilis*, *L. monocytogenes* and *E. faecalis*. Pie charts indicate the number of regulators identified in each functional category and organism (Tables S2-S5). (**D-I**) Examples of novel regulatory elements (yellow arrows) identified in this study. Axes and colors are as in Fig. 1E.

Europe PMC Funders Author Manuscripts

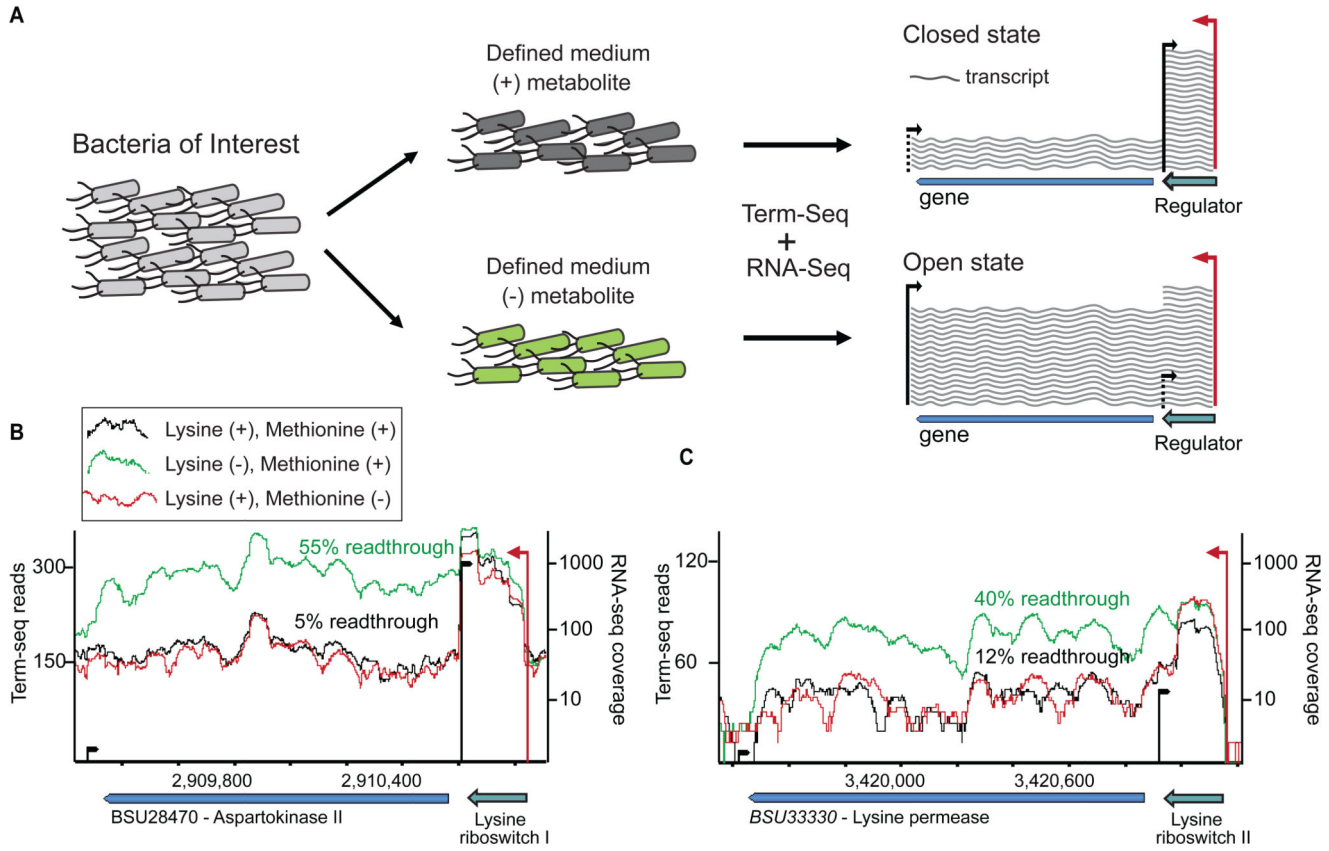

Fig. 3. *In-vivo* metabolite screening using RNA sequencing.

(**A**) Genome-wide experimental approach for *in-vivo* screening of termination-based regulators that respond to a metabolite of choice in physiological conditions. A bacterium of interest is cultured in a defined medium with or without the metabolite of choice. After a brief incubation, RNA is extracted and sequenced using term-seq and RNA-seq. The long/short transcript ratio, indicative of the open/closed state of the regulator, can be calculated from term-seq or RNA-seq counts. (**B**-**C**) *B. subtilis* was grown in defined, minimal media either containing both lysine and methionine (black RNA-seq coverage), lacking lysine and containing methionine (green) or containing lysine and lacking methionine (red). RNA-seq coverage was normalized by the number of uniquely mapped reads in each sequencing library.

Europe PMC Funders Author Manuscripts

Europe PMC Funders Author Manuscripts

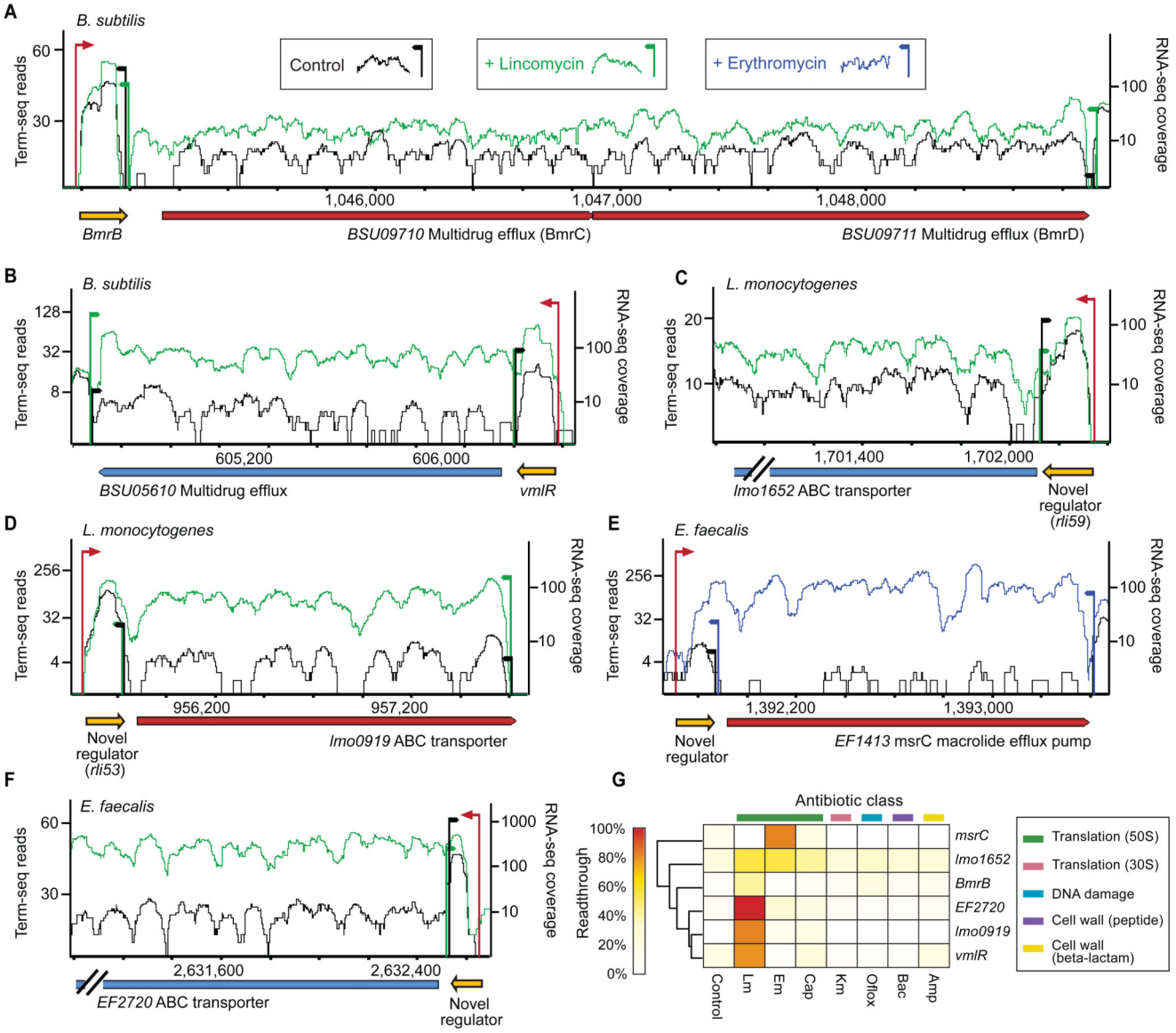

Fig. 4. Antibiotic responsive conditional terminators.

The antibiotic-dependent response of known and novel regulators as measured *in-vivo* by term-seq and RNA-seq. Black, green and blue RNA-seq coverage and term-seq sites denote the control (LB), lincomycin, and erythromycin conditions, respectively. Term-seq sites represent average read coverage across 3 biological replicates. (**A**) The *B. subtilis bmrCD* operon. (**B**) The *B. subtilis vmlR* gene. (**C**-**F**) Antibiotic dependent transcriptional read-through in novel regulators discovered in *L. monocytogenes* and *E. faecalis*. (**G**) Condition-specific read-through calculated in the control and the seven antibiotics exposure experiments. The antibiotic class is defined by the cellular process/component targeted. RNA-seq was normalized as in Fig. 3. Antibiotics and abbreviations used: Lincomycin (Lm), Erythromycin (Em), Chloramphenicol (Cap), Kanamycin (Km), Ofloxacin (Oflox), Bacitracin (Bac) and Ampicillin (Amp).

Europe PMC Funders Author Manuscripts

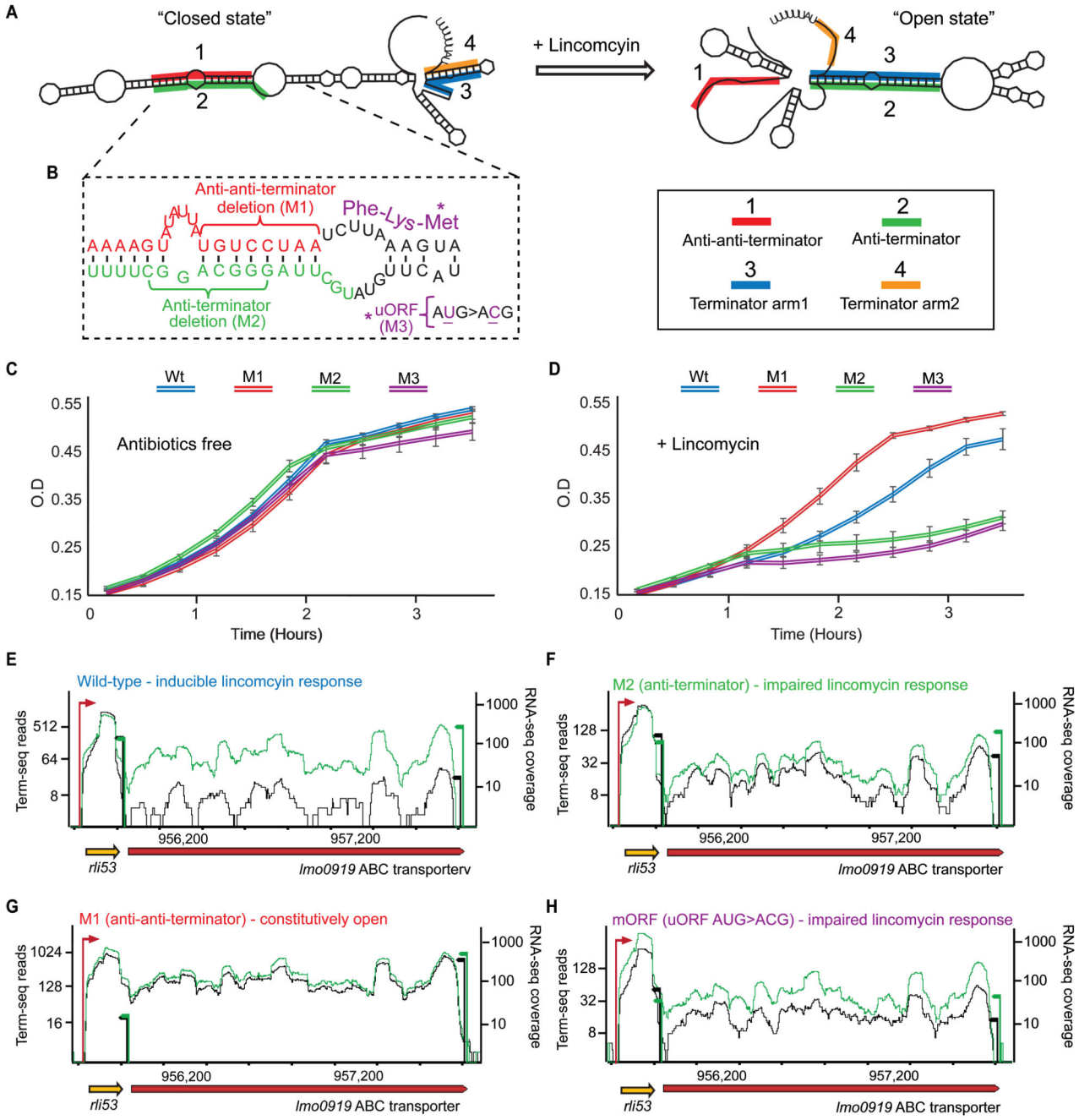

Fig. 5. Antibiotic-responsive terminator/antiterminator RNA structures control the expression of *lmo0919*.

Mutational analysis of the 5'UTR of *lmo0919* provides insights into the mechanism of inducible antibiotic resistance. (**A**) A predicted RNA secondary structure of the *lmo0919* 5' UTR. This element is predicted to form two alternative, mutually exclusive structures that mediate either termination or antibiotic-dependent read-through. Left, the "closed-state" structure encodes a terminator and an upstream stem; right, the "open-state" structure in which the terminator structure is sequestered by an anti-terminator. (**B**) Generation of

mutants that interrupt the anti-anti-terminator (red), the anti-terminator (green), or a conserved uORF that overlaps the anti-anti-terminator (purple). (**C**-**D**). Mutants were grown in BHI media without lincomycin (**C**) or containing 0.5ug/ml lincomycin (**D**), respectively. Error bars represent standard error. (**E**-**H**) Term-seq and RNA-seq coverage of WT and mutants grown in BHI without lincomycin (black RNA-seq curves and black term-seq sites) or with 0.5ug/ml lincomycin (green RNA-seq curves and green term-seq sites). RNA-seq coverage was normalized as in Fig 3.

Europe PMC Funders Author Manuscripts

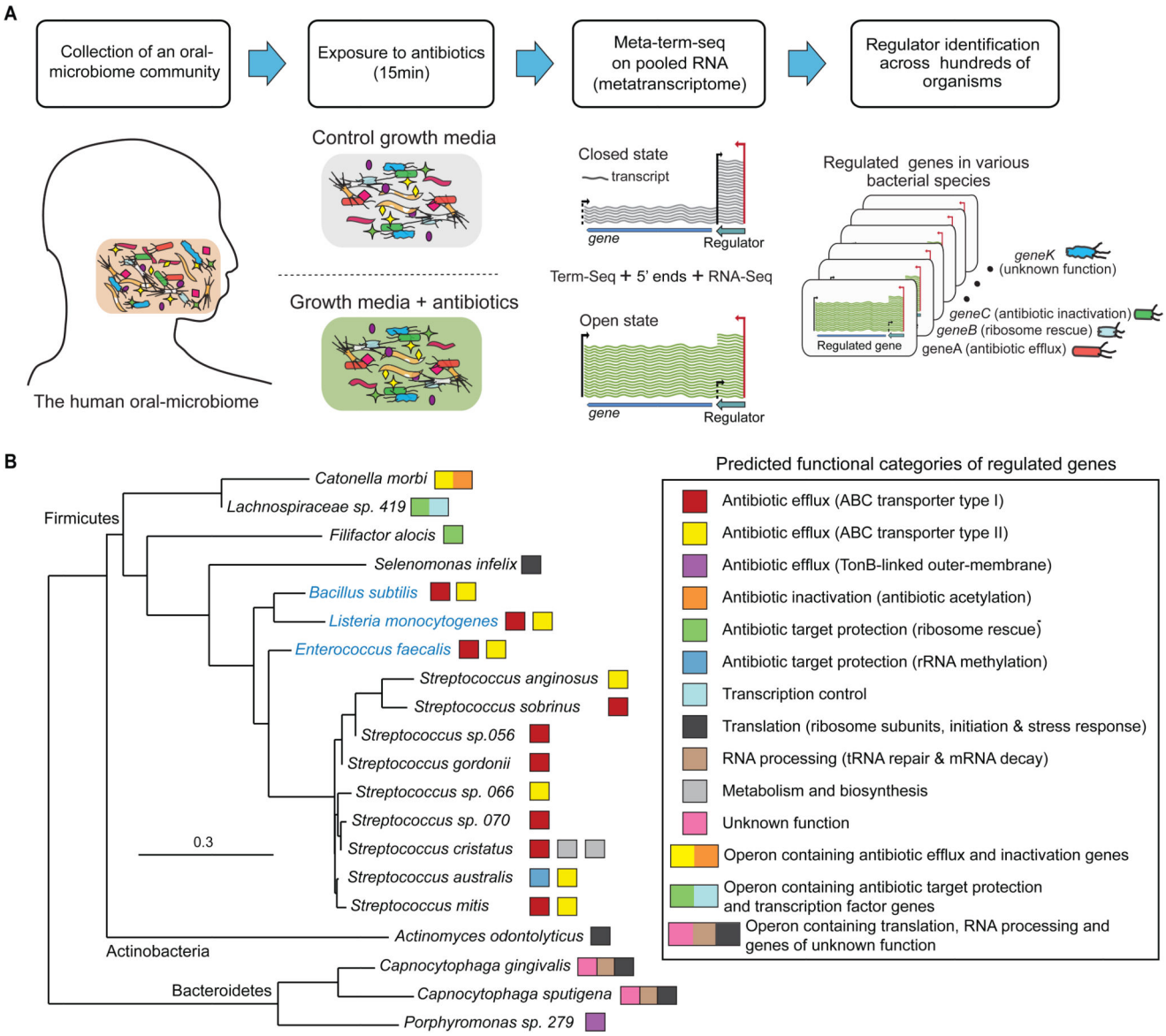

Fig. 6. Antibiotic-responsive ribo-regulation in the human oral microbiome.

The meta-term-seq approach facilitates the discovery of metabolite-responsive regulators across complex bacterial communities. (**A**) Schematics of the meta-term-seq workflow from sample collection to regulator identification. (**B**) A 16S rRNA phylogenetic tree comprised of oral microbiome bacteria found to have one or more lincomycin-responsive regulators (23). The predicted functions of the regulated genes in each species are indicated by colored boxes according to the inset legend. In some cases a single operon contained several different functions (multi-colored rectangles, legend bottom). Individual bacteria studied in monoculture were added to the tree (marked by blue-colored names).